EUROPEAN ORGANIZATION FOR NUCLEAR RESEARCH

L3 Note 2587
July 7, 2000

Searches for Scalar Quarks in e^+e^- Interactions at $\sqrt{s} = 192 - 202$ GeV

The L3 Collaboration

Abstract

Searches for scalar top and scalar bottom quarks, as well as for mass-degenerate scalar quarks of the first two families are performed at 192–202 GeV centre-of-mass energy with the L3 detector at LEP. No signals are observed. Model-independent limits on the scalar top production cross sections are determined for the decay modes $\tilde{t}_1 \to c\tilde{\chi}^0_1$ and $\tilde{t}_1 \to b\ell\tilde{\nu}$. For scalar quarks of the other flavours $\tilde{q} \to q\tilde{\chi}^0_1$ decays are considered. Within the framework of the Minimal Supersymmetric Standard Model mass limits are set at 95% C.L. for these particles. Indirect limits on the gluino mass are also derived.

Submitted to *XXXth International Conference on High Energy Physics*
Osaka, Japan, 27 July – 2 August 2000

1 Introduction

In the Minimal Supersymmetric extension of the Standard Model (MSSM) [1] for each helicity state of Standard Model (SM) quarks, $\mathrm{q}_{\mathrm{L,R}}$, there is a corresponding scalar SUSY partner $\tilde{\mathrm{q}}_{\mathrm{L,R}}$. Generally, the left, $\tilde{\mathrm{q}}_{\mathrm{L}}$, and right, $\tilde{\mathrm{q}}_{\mathrm{R}}$, eigenstates mix to form mass eigenstates. The mixing is proportional to the corresponding SM quark mass and to the parameter $a_{\mathrm{q}} = A_{\mathrm{q}} - \mu \cot\beta$ for up type quarks and $a_{\mathrm{q}} = A_{\mathrm{q}} - \mu \tan\beta$ for down type ones. A_{q} is the trilinear coupling among scalars, μ the Higgsino mass parameter and $\tan\beta$ the ratio of the vacuum expectation values of the two Higgs fields. For the first two generations of scalar quarks (squarks) the weak eigenstates are also mass eigenstates to a good approximation. However, this does not hold for the squarks of the third family. Due to the heavy top quark the $\tilde{\mathrm{t}}_{\mathrm{L}} - \tilde{\mathrm{t}}_{\mathrm{R}}$ mixing is enhanced, leading to a large splitting between the two mass eigenstates. This is usually expressed in terms of the mixing angle, θ_{LR}. The lighter scalar top (stop) quark

$$\tilde{\mathrm{t}}_1 = \tilde{\mathrm{t}}_{\mathrm{L}} \cos\theta_{\mathrm{LR}} + \tilde{\mathrm{t}}_{\mathrm{R}} \sin\theta_{\mathrm{LR}} \tag{1}$$

can thus be well within the discovery range of LEP. Furthermore, if $\tan\beta \gtrsim 10$, large $\tilde{\mathrm{b}}_{\mathrm{L}} - \tilde{\mathrm{b}}_{\mathrm{R}}$ mixing occurs. This may lead to a scalar bottom (sbottom) quark, $\tilde{\mathrm{b}}_1$, also light enough to be accessible at LEP.

In the present analysis, R-parity conservation is assumed, which implies that SUSY particles (sparticles) are produced in pairs; heavier sparticles decay into lighter ones and the Lightest Supersymmetric Particle (LSP) is stable. In the MSSM the best LSP candidate is the weakly interacting lightest neutralino, $\tilde{\chi}^0_1$.

Squark pair production at LEP proceeds via the exchange of Z/γ bosons in the s-channel. The production cross section is governed by two free parameters: the squark mass and the mixing angle, θ_{LR} [2]. At $\cos\theta_{\mathrm{LR}} \sim 0.57$ the stop decouples from the Z and the cross section is minimal. The corresponding value is $\cos\theta_{\mathrm{LR}} \sim 0.39$ for the sbottom. The cross section reaches the maximum at $\cos\theta_{\mathrm{LR}}$=1 when the light squark mass eigenstate is the weak eigenstate.

At LEP energies the most important stop decay channels are: $\tilde{\mathrm{t}}_1 \to \mathrm{c}\tilde{\chi}^0_1$, $\mathrm{b}\nu_\ell\tilde{\ell}$, $\mathrm{b}\ell\tilde{\nu}_\ell$, and $\mathrm{b}\tilde{\chi}^+_1$, where the $\tilde{\ell}$ and $\tilde{\nu}_\ell$ are the supersymmetric partners of the charged leptons and neutrinos, and the $\tilde{\chi}^0_1$ and $\tilde{\chi}^+_1$ are the lightest neutralino and chargino, respectively. The $\tilde{\mathrm{t}}_1 \to \mathrm{b}\tilde{\chi}^\pm_1$ decay channel is the dominant one when kinematically allowed. However, the current limits on the chargino mass [3] preclude this decay to occur, except for a small region in the MSSM parameter space with the common scalar mass (m_0) from 60 to 90 GeV. Similarly, the $\tilde{\mathrm{t}}_1 \to \mathrm{b}\nu_\ell\tilde{\ell}$ decay is precluded by the current limits [3] on charged scalar lepton masses. The stop analysis is performed considering the $\tilde{\mathrm{t}}_1 \to \mathrm{c}\tilde{\chi}^0_1$ and $\tilde{\mathrm{t}}_1 \to \mathrm{b}\ell\tilde{\nu}_\ell$ decay channels, with $\tilde{\nu}_\ell$ decaying invisibly $\tilde{\nu}_\ell \to \nu_\ell\tilde{\chi}^0_1$. Since the $\tilde{\mathrm{t}}_1 \to \mathrm{c}\tilde{\chi}^0_1$ is a flavour changing weak decay, the $\tilde{\mathrm{t}}_1 \to \mathrm{b}\ell\tilde{\nu}_\ell$ channel is dominant when kinematically allowed. Therefore the two decay modes are investigated each with the assumption of 100% branching fraction. For the stop three-body decay channel $\tilde{\mathrm{t}}_1 \to \mathrm{b}\ell\tilde{\nu}_\ell$, two scenarios are considered: ℓ being e, μ or τ with equal probabilities or pure τ. The latter occurs at high $\tan\beta$ values.

For sbottom, as well as for the first two generations of squarks, the $\tilde{\mathrm{q}} \to \mathrm{q}\tilde{\chi}^0_1$ decay mode is investigated under the assumption of 100% branching fraction.

Since the stop two-body decay $\tilde{\mathrm{t}}_1 \to \mathrm{c}\tilde{\chi}^0_1$ is a second order weak decay, the lifetime of the $\tilde{\mathrm{t}}_1$ is larger than the typical hadronisation time of 10^{-23}s. The $\tilde{\mathrm{t}}_1 \to \mathrm{b}\ell\tilde{\nu}$ decay proceeds via a virtual chargino exchange and the lifetime is also expected to be larger than the hadronisation time. Thus the stop will first hadronise and then decay. For the sbottom the situation depends on the gaugino-higgsino content of the neutralino: for a gaugino-like neutralino the sbottom lifetime is expected to be larger than the hadronisation time. In the present analysis a 'hadronisation before decay' scenario is followed. Although hadronisation does not change the final event topology, it affects the track multiplicity, the jet properties and the event shape.

The present study supersedes previous L3 limits on stop and sbottom quark productions [4]. Searches for supersymmetric quarks have been performed by other LEP [5] and by TEVATRON [6, 7] experiments.

2 Data Samples and Simulation

The data used in the present analysis were collected in 1999 at centre of mass eneries of $\sqrt{s}$=192, 196, 200 and 202 GeV using the L3 detector [8]. The corresponding integrated luminosities amount to 29.7 pb^{-1}, 83.7 pb^{-1}, 81.7 pb^{-1} and 37.0 pb^{-1}, respectively.

Monte Carlo (MC) samples of squark events are generated using a PYTHIA based event generator [9]. The squark mass has been varied from 45 GeV up to the kinematical limit and the $\tilde{\chi}^0_1$ mass from 1 GeV to $M_{\tilde{\mathrm{t}}_1}-2$ GeV or to $M_{\tilde{\mathrm{b}}_1}-5$ GeV for the stop and sbottom two-body decay modes. The $\tilde{\mathrm{t}}_1 \rightarrow \mathrm{b}\ell\tilde{\nu}$ and $\tilde{\mathrm{t}}_1 \rightarrow \mathrm{b}\tau\tilde{\nu}$ channels are generated with $\tilde{\nu}$ mass from 43 GeV to $M_{\tilde{\mathrm{t}}_1} - 7$ GeV.

The following MC programs are used to estimate the Standard Model backgrounds: PYTHIA [10] for $\mathrm{e}^+\mathrm{e}^- \rightarrow \mathrm{q}\bar{\mathrm{q}}$, $\mathrm{e}^+\mathrm{e}^- \rightarrow \mathrm{ZZ}$ and $\mathrm{e}^+\mathrm{e}^- \rightarrow \mathrm{Ze}^+\mathrm{e}^-$, KORALZ [11] for $\mathrm{e}^+\mathrm{e}^- \rightarrow \tau^+\tau^-$, KORALW [12] for $\mathrm{e}^+\mathrm{e}^- \rightarrow \mathrm{W}^+\mathrm{W}^-$, EXCALIBUR [13] for $\mathrm{e}^+\mathrm{e}^- \rightarrow \mathrm{W}^\pm\mathrm{e}^\mp\nu$, PHOJET [14] for $\mathrm{e}^+\mathrm{e}^- \rightarrow \mathrm{e}^+\mathrm{e}^-\mathrm{q}\bar{\mathrm{q}}$ and DIAG36 [15] for $\mathrm{e}^+\mathrm{e}^- \rightarrow \mathrm{e}^+\mathrm{e}^-\tau^+\tau^-$. The number of simulated events for each background process exceeds by 100 times the statistics of the collected data samples except for the two-photon collision processes, for which the MC statistics amounts to only twice the data.

The response of the L3 detector is simulated using the GEANT 3.15 package [16]. It takes into account effects of energy loss, multiple scattering and showering in the detector materials and in the beam pipe. Hadronic interactions are simulated with the GHEISHA program [17].

3 Event Preselection

The signal events of $\tilde{\mathrm{t}}_1 \rightarrow \mathrm{c}\tilde{\chi}^0_1$ and $\tilde{\mathrm{b}}_1 \rightarrow \mathrm{b}\tilde{\chi}^0_1$ contain two high multiplicity acoplanar jets originated from c or b-quarks. In addition, two charged leptons are present in the $\tilde{\mathrm{t}}_1 \rightarrow \mathrm{b}\ell\tilde{\nu}$ decay channel. The neutralinos and sneutrinos in the final state escape detection leading to missing energy in the event. A common preselection is applied to obtain a sample of unbalanced hadronic events. The events have to fulfil the following requirements: more than four tracks; at least 10 but not more than 40 calorimetric clusters; a visible energy, E_{vis}, between 5 GeV and 150 GeV; an energy deposition in the forward calorimeters less than 10 GeV and a total energy in the 30° cone around the beam pipe less than $0.25\times E_{\mathrm{vis}}$; a transverse missing momentum, $P_{\mathrm{T}}^{\mathrm{miss}}$, greater than 2 GeV and a sinus of the polar angle of the missing momentum, $\sin\theta_{\mathrm{miss}}$, greater than 0.2.

After the preselection 4136 events are retained, compared with 4765 ± 25 expected from the SM processes, which are dominated by two-photon interactions. Figure 1 shows the distributions of E_{vis}; $E_{\mathrm{TTJ}}/P_{\mathrm{T}}^{\mathrm{miss}}$, where $E_{\mathrm{TTJ}}$is the absolute value of the total momentum of the two jets projected onto the direction perpendicular to the thrust axis computed in the transverse plane; the energy of the most energetic lepton, E_ℓ and the b-tagging event discriminant, D_{Btag}. D_{Btag} is defined as the negative log-likelihood of the probability for the event to be consistent with light quark production [18]. After preselection the data and MC are in good agreement. The discrepancy in the total number of data and MC events is localised in the low $E_{\rm vis}$ region, which is dominated by two-photon processes. This effect is taken into account by assigning a systematic error of 10–20% on the two-photon cross section.

4 Selection Optimisation

The kinematics of the signal events strongly depend on the mass difference between squark and neutralino, $\Delta M = M_{\tilde{\rm q}} - M_{\tilde{\chi}^0_1}$. In the very low ΔM region, the visible energy and track multiplicity are low. Therefore, signal events are difficult to separate from the two-photon interactions. For high ΔM values, signal events will be similar to $\rm W^+W^-$, $\rm W^\pm e^\mp \nu$ or ZZ final states. The most favourable region for the signal and background separation is expected at ΔM=20–40 GeV.

To cope with the various background sources, the searches are performed independently in different ΔM regions. For $\tilde{\rm t}_1 \rightarrow {\rm c}\tilde{\chi}^0_1$ and $\tilde{\rm b}_1 \rightarrow {\rm b}\tilde{\chi}^0_1$ decays four selections have been optimised. These selections typically cover ΔM regions of: 5–10 GeV, 10–20 GeV, 20–40 GeV and $\gtrsim$ 40 GeV. In case of $\tilde{\rm t}_1 \rightarrow {\rm b}\ell\tilde{\nu}$ decays three selections are devised for each lepton flavour. These selections cover the $\Delta M = M_{\tilde{\rm q}} - M_{\tilde{\nu}}$ region consistent with the limit $M_{\tilde{\nu}} \gtrsim 43$ GeV from LEP1 [19].

The following kinematic variables are used in the selections: Lower cuts on $E_{\rm vis}$, $P_{\rm T}^{\rm miss}$ and $P_{\rm T}^{\rm miss}/E_{\rm vis}$ separate signal from two-photon background, whereas an upper cut on $E_{\rm vis}$ removes $\rm W^+W^-$, $\rm W^\pm e^\mp \nu$, ZZ and $\rm Ze^+e^-$ events. A cut on $\sin\theta_{\rm miss}$ rejects $\rm e^+e^-q\bar{q}$ events. Cuts on jet acollinearity and acoplanarity reduce the $\rm q\bar{q}$ contribution. A veto on the energy deposition in the 50° azimuthal sector around the missing momentum direction suppresses $\tau^+\tau^-$ and $\rm q\bar{q}$ events. The $\rm W^+W^-$ production, where one W decays leptonically and $\rm W^\pm e^\mp \nu$ events are removed by vetoing energetic isolated leptons. The cut on $E_{\rm TTJ}$ suppresses $\rm e^+e^-q\bar{q}$, $\rm q\bar{q}$ as well as $\rm W^+W^-$ backgrounds.

For the selections of $\tilde{\rm b}_1 \rightarrow {\rm b}\tilde{\chi}^0_1$ and $\tilde{\rm t}_1 \rightarrow {\rm b}\ell\tilde{\nu}$ signal events, cuts are applied on the event b-tagging variable $D_{\rm Btag}$.

At least one isolated lepton is required in the case of $\tilde{\rm t}_1 \rightarrow {\rm b}\ell\tilde{\nu}$ decays. An electron is isolated if the calorimetric energy deposition in a 10° cone around its direction is less than 2 GeV. Muon isolation requirement implies an energy deposition in the cone between 5° to 10° around its direction of less than 2 GeV. A tau is isolated when the calorimetric energy deposition in the cone between 10° to 20° around its direction is less than 2 GeV and less than 50% of the tau energy. Furthermore, the energy deposition in a cone between 20° to 30° must be less than 60% of the tau energy. Finally, a lower cut on the energy of the most energetic lepton in the event is applied in order to suppress mainly the two-photon and the $\rm q\bar{q}$ backgrounds.

The cut values on the kinematic variables are chosen by an optimisation procedure for the different ΔM regions. The procedure minimises the average limit for an infinite number of trials assuming only background contributions [20]. For each signal mass point, the optimal selection or combination of selections is chosen.

The expected signal efficiencies for a 90 GeV stop and sbottom at various ΔM values are given in Table 1 together with the SM background expectations at $\sqrt{s} = 196$ GeV.

5 Systematic Errors

The main systematic errors on the signal selection efficiency arise from the uncertainties in the squark production, hadronisation and decay scheme. These effects are evaluated in the similar manner as in Reference [4]. The overall relative systematic error on the selection efficiencies ranges from 7% to 16% and from 7% to 11% for stop and sbottom, respectively. This error and the uncertainty on the background normalisation, dominated by MC statistics, as well as the quoted uncertainty on two-photon background, are incorporated in the final results following to the method of Reference [21].

6 Results

Table 2 summarises the number of selected data and expected background events with different ΔM selections for all investigated channels separately for four centre of mass energies $\sqrt{s}$=192, 196, 200, 202 GeV and for total $\sqrt{s}$ =192–202 GeV sample. The total number of observed candidates in the $\tilde{\mathrm{t}}_1 \rightarrow \mathrm{c}\tilde{\chi}^0_1$ and $\tilde{\mathrm{b}}_1 \rightarrow \mathrm{b}\tilde{\chi}^0_1$ channels are 66 and 42, compared to 82.1 $\pm$ 5.1 and 44.8 $\pm$ 4.2 events expected from the SM processes. In the $\tilde{\mathrm{t}}_1 \rightarrow \mathrm{b}\ell\tilde{\nu}$ and $\tilde{\mathrm{t}}_1 \rightarrow \mathrm{b}\tau\tilde{\nu}$ channels 46 and 25 events have been selected, wheras the SM expectations are 41.0 $\pm$ 4.0 and 36.3 $\pm$ 3.8 events.

The composition of the expected background into two-fermion, four-fermion and two-photon processes is given in Table 3. When all the ΔM selections for all investigated channels are applied, 129 events are retained. This is consistent with 136.7 $\pm$ 6.9 events expected from SM processes, mainly due to two-photon interactions. Thus no evidence for stop or sbottom is found and upper limits are derived on their production cross sections.

Model-independent cross section limits in the $M_{\tilde{\mathrm{q}}}$, $M_{\tilde{\chi}^0_1}$ plane are given in Figure 2 for stop and sbottom assuming 100% branching fraction for the $\tilde{\mathrm{t}}_1 \rightarrow \mathrm{c}\tilde{\chi}^0_1$ and $\tilde{\mathrm{b}}_1 \rightarrow \mathrm{b}\tilde{\chi}^0_1$ decays. The limits are obtained by combining the present results with those obtained at $\sqrt{s} = 161 - 172$ GeV, 183 GeV [22] and $\sqrt{s}$=189 GeV [4]. The evaluated limits correspond to luminosity weighted average cross sections. In the medium ΔM region cross sections larger than 0.05 pb are excluded.

The cross section limits for stop production assuming $\tilde{\mathrm{t}}_1 \rightarrow \mathrm{b}\ell\tilde{\nu}$ decay, in the two scenarios for lepton flavours, ℓ=e, μ, τ with equal probability or $\ell=\tau$, are given in Figure 3. Cross sections larger than 0.05 pb are excluded in big portion of $(M_{\tilde{\mathrm{q}}}, M_{\tilde{\nu}})$ mass plane.

7 MSSM Interpretation

In the MSSM the stop and sbottom production cross sections depend on the squark mass and the mixing angle $\cos\theta_{\mathrm{LR}}$. Comparing the theoretical prediction with the 95% C.L. limit on the production cross section, we determine the excluded mass regions for $\tilde{\mathrm{t}}_1$ and $\tilde{\mathrm{b}}_1$. Figure 4a shows the excluded $\tilde{\mathrm{t}}_1$ mass region as a function of $M_{\tilde{\mathrm{t}}_1}$ and $M_{\tilde{\chi}^0_1}$ at $\cos\theta_{\mathrm{LR}}$=1 and 0.57 for the $\tilde{\mathrm{t}}_1 \rightarrow \mathrm{c}\tilde{\chi}^0_1$ decay. For this decay mode, stop masses below 91 GeV are excluded under the assumptions of $\Delta M = M_{\tilde{\mathrm{t}}_1} - M_{\tilde{\chi}^0_1}$ greater than 15 GeV and $\cos\theta_{\mathrm{LR}}$=1. For the same values of ΔM and in the most pessimistic scenario of $\cos\theta_{\mathrm{LR}}$=0.57, the mass limit is 88 GeV. The region where $\tilde{\mathrm{t}}_1 \rightarrow \mathrm{bW}\tilde{\chi}^0_1$ decay is kinematically accessible and becoming the dominant decay mode, is also indicated. This decay is not considered in the analysis.

The exclusion plot for the sbottom is given in Figure 4b for $\cos\theta_{\mathrm{LR}}$=1 and $\cos\theta_{\mathrm{LR}}$=0.39. Sbottom masses below 94 GeV are excluded assuming ΔM greater than 15 GeV and $\cos\theta_{\mathrm{LR}}$=1. In the most pessimistic scenario of $\cos\theta_{\mathrm{LR}}$=0.39, the mass limit obtained is 80 GeV.

The excluded stop mass regions, if the dominant three-body decays are kinematically open, are given in Figure 5. Figure 5a corresponds to $\tilde{\mathrm{t}}_1 \rightarrow \mathrm{b}\ell\tilde{\nu}$, ℓ=e, μ, τ with equal probability. Here the lower $\tilde{\mathrm{t}}_1$ mass limits are 95 GeV and 91.5 GeV for $\cos\theta_{\mathrm{LR}}$=1 and 0.57, respectively. The corresponding exclusion limits for stop decays through $\tilde{\mathrm{t}}_1 \rightarrow \mathrm{b}\tau\tilde{\nu}$ are shown in Figure 5b. Mass limits of 93 GeV and 90 GeV are obtained, assuming $\Delta M >$15 GeV.

For a fixed value of ΔM =15 GeV the excluded stop and sbottom masses as a function of the mixing angle are shown in Figure 6. The exclusion limits mainly reflect the cross section behaviour. At $\cos\theta_{\mathrm{LR}}$=1, the $\tilde{\mathrm{t}}_1$ and $\tilde{\mathrm{b}}_1$ cross sections are quite similar. As $\cos\theta_{\mathrm{LR}}$ decreases squark production proceeds mainly via γ exchange rendering the sbottom production cross section about 4 times lower than that of the stop. Consequently, the sbottom exclusion limits are relatively modest at low $\cos\theta_{\mathrm{LR}}$ values.

For squarks of the first two generations, the same selection efficiencies are assumed as for the stop two-body decays, because of the similar event topologies (jets and missing energy). Then the cross section limits given in Figure 2a are interpreted in terms of degenerate squark masses. Figure 7a shows the squark mass limit as a function of the LSP mass. Two scenarios are considered: "left" and "right" squark degeneracy or only "right" squark production. In the first case, with four degenerate squark flavours, the mass limit is set at 96.5 GeV for ΔM greater than 10 GeV. In the case of only "right" squark production, the mass limit is 93 GeV.

Assuming gaugino unification at the GUT scale, the results on the four degenerate squarks are reinterpreted on the $M_{\tilde{\mathrm{g}}}$, $M_{\tilde{\mathrm{q}}}$ plane as shown in Figure 7b. Moreover, the gaugino unification allows a transformation of the absolute limit on M_2, obtained from the chargino, neutralino and scalar lepton searches [23, 24], into a limit on the gluino mass as shown in Figure 7b. This is done using the ISAJET program [25]. For $\tan\beta = 4$, gluino masses up to about 250$-$295 GeV are excluded at 95% C.L.

Acknowledgements

We thank S. Kraml for many useful discussions and comments. We wish to express our gratitude to the CERN accelerator division for the excellent performance of the LEP machine. We acknowledge the effort of those engineers and technicians who have participated in the construction and maintenance of this experiment.

References

[1] For a review see, *e.g.* H.E. Haber and G.L. Kane, Phys. Rep. **117** (1985) 75.

[2] A. Bartl *et al.*, Z.Phys **C 73** (1997) 469.

[3] I. Iashvili, *MSSM SUSY Searches at LEP2* presentation at XXXV Rencontres de Moriond, Electroweak Interactions and Unified Theories, Les Arcs, March 11-18, 2000.

[4] L3 Collaboration, M. Acciarri *et al.*, Phys. Lett. **B 471** (1999) 308.

[5] *Search for sleptons and squarks in e+ e- collisions at* $\sqrt(s) = 188.6$ *GeV*, ALEPH Collaboration, R. Barate *et al.*, ALEPH 99-067 CONF;
Search for supersymmetric partners of top and bottom quarks at $\sqrt(s) = 189$ *GeV*, DELPHI Collaboration, P. Abreu *et al.*, DELPHI 99-74 CONF 261;
OPAL Collaboration, G. Abbiendi *et al.*, Phys. Lett. **B 456** (1999) 95.

[6] The CDF Collaboration, T. Affolder *et al.*, Phys. Rev. Lett. **84** (2000) 5704.

[7] Phys. Rev. Lett. **76** (1996) 2222.

[8] The L3 Collaboration, B. Adeva *et al.*, Nucl. Instr. and Meth. **A 289** (1990) 35;
M. Chemarin *et al.*, Nucl. Instr. and Meth. **A 349** (1994) 345;
M. Acciarri *et al.*, Nucl. Instr. and Meth. **A 351** (1994) 300;
G. Basti *et al.*, Nucl. Instr. and Meth. **A 374** (1996) 293;
I.C. Brock *et al.*, Nucl. Instr. and Meth. **A 381** (1996) 236;
A. Adam *et al.*, Nucl. Instr. and Meth. **A 383** (1996) 342.

[9] Modified version of OPAL MC generator for squarks production, E. Accomodo *et al.*,, 'Physics at LEP2', eds. G. Altarelli, T. Sjöstrand and F. Zwirner, CERN 96-01, vol. 2, 286; paper in preparation..

[10] T. Sjöstrand, `PYTHIA 5.7` and `JETSET 7.4` Physics and Manual, CERN-TH/7112/93 (1993), revised August 1995; Comp. Phys. Comm. **82** (1994) 74.

[11] S. Jardach, B.F.L. Ward, and Z. Wąs, Comp. Phys. Comm. **79** (1994) 503.
Version 4.02 was used.

[12] M. Skrzypek *et al.*, Comp. Phys. Comm. **94** (1996) 216;
M. Skrzypek *et al.*, Phys. Lett. **B 372** (1996) 289.
Version 1.21 was used.

[13] F.A. Berends, R. Kleiss, and R. Pittau, Nucl. Phys. **B 424** (1994) 308; Nucl. Phys. **B 426** (1994) 344; Nucl. Phys. (Proc. Suppl.) **B 37** (1994) 163; Phys. Lett. **B 335** (1994) 490; Comp. Phys. Comm. **85** (1995) 447.

[14] R. Engel, Z. Phys. **C 66** (1995) 203; R. Engel and J. Ranft, Phys. Rev. **D 54** (1996) 4244.
Version 1.05 was used.

[15] F.A. Berends, P.H. Daverfeldt and R. Kleiss, Nucl. Phys. **B 253** (1985) 441.

[16] R. Brun *et al.*, CERN DD/EE/84-1 (Revised 1987).

[17] H. Fesefeldt, RWTH Aachen Report PITHA 85/2 (1985).

[18] L3 Collaboration, M. Acciarri *et al.*, Phys. Lett. **B 411** (1997) 373..

[19] C. Caso *et al.*, Eur. Phys. J. **C 3** (1998) 1.

[20] J.F. Grivaz and F. Le Diberder, preprint LAL-92-37, June 1992.

[21] R.D. Cousins and V.L. Highland, Nucl. Inst. Meth. **A 320** (1992) 331.

[22] L3 Collaboration, M. Acciarri *et al.*, Phys. Lett. **B 445** (1999) 428.

[23] L3 Collaboration, *Search for Scalar Leptons and Quarks in* e^+e^- *collisions at* $\sqrt{s} = 192 - 202$ *GeV* , L3 Note 2524, submitted to Winter 2000 Conferences.

[24] L3 Collaboration, *Searches for Charginos and Neutralinos in* e^+e^- *Collisions at* $\sqrt{s} = 192 - 202$ *GeV*, L3 Note 2522, submitted to Winter 2000 Conferences.

[25] H. Baer *et al.*, in Proceedings of the Workshop on Physics at Current Accelerators and Supercolliders, ed. J. Hewett and D. Zeppenfeld (Argonne National Laboratory, Argonne, Illinois, 1993).

[26] Phys.Rev.Lett. **84** (2000) 5273.

[27] CDF Collaboration, F. Abe *et al.*, Phys. Rev. **D 56** (1997) 1357;
D0 Collaboration, S. Abachi *et al.*, Phys. Rev. Lett. **75** (1995) 618..

[28] UA1 Collaboration, C. Albajar *et al.*, Phys. Lett. **B 198** (1987) 261;
UA2 Collaboration, J. Alitti *et al.*, Phys. Lett. **B 235** (1990) 363.

Table 1: Selection efficiencies, ϵ, and number of expected events from SM processes, N_{SM}, for a 90 GeV stop and sbottom, as a function of ΔM (see text).

ΔM (GeV)	$\tilde{t}_1 \to c\tilde{\chi}_1^0$		$\tilde{t}_1 \to b\ell\tilde{\nu}$		$\tilde{t}_1 \to b\tau\tilde{\nu}$		$\tilde{b}_1 \to b\tilde{\chi}_1^0$	
	ϵ (%)	N_{SM}	ϵ (%)	N_{SM}	ϵ (%)	N_{SM}	ϵ (%)	N_{SM}
5	20.0	19.20	-	-	-	-	?	?
7	23.2	22.5	25.5	11.0	7.8	6.80	6.9	2.02
10	17.8	3.30	40.8	14.8	19.2	12.8	17.2	2.02
20	44.3	6.10	58.9	4.52	42.3	6.75	38.6	2.20
30	52.8	3.25	48.2	0.61	37.2	1.40	41.2	0.57
40	37.0	3.25	39.3	0.61	35.5	1.40	37.9	1.11
47	43.1	7.18	33.0	0.61	34.3	1.40	34.5	1.11
60	30.0	3.93	-	-	-	-	28.2	1.11
80	35.5	3.93	-	-	-	-	23.0	0.52
88	32.9	3.93	-	-	-	-	24.2	0.58

Table 2: Number of observed events, N_{D}, and SM background expectations, N_{SM}, for the stop and sbottom selections at very low (5–10 GeV), low (10–20 GeV), medium (20–40 GeV) and high ($\gtrsim$ 40 GeV) ΔM. The quoted errors are due to MC statistics only.

Selection	$\tilde{\mathrm{t}}_1 \to \mathrm{c}\tilde{\chi}^0_1$		$\tilde{\mathrm{t}}_1 \to \mathrm{b}\ell\tilde{\nu}$		$\tilde{\mathrm{t}}_1 \to \mathrm{b}\tau\tilde{\nu}$		$\tilde{\mathrm{b}}_1 \to \mathrm{b}\tilde{\chi}^0_1$	
	N_{D}	N_{SM}	N_{D}	N_{SM}	N_{D}	N_{SM}	N_{D}	N_{SM}
Very low ΔM	6	6.83 ± 0.60	3	3.90 ± 0.46	5	2.39 ± 0.36	4	4.79 ± 0.50
Low ΔM	0	1.11 ± 0.20	2	1.35 ± 0.26	3	2.01 ± 0.31	0	0.68 ± 0.18
Medium ΔM	2	1.10 ± 0.14	0	0.132 ± 0.025	0	0.47 ± 0.13	0	0.149 ± 0.057
High ΔM	3	1.23 ± 0.07	-	-	-	-	0	0.124 ± 0.023
Combined	11	10.06 ± 0.65	5	5.24 ± 0.52	8	4.58 ± 0.48	4	5.65 ± 0.53
Very low ΔM	14	19.2 ± 1.7	14	11.0 ± 1.3	5	6.8 ± 1.0	15	13.5 ± 1.4
Low ΔM	1	3.30 ± 0.59	2	4.10 ± 0.76	1	6.19 ± 0.93	0	2.02 ± 0.53
Medium ΔM	2	3.25 ± 0.42	0	0.61 ± 0.22	0	1.40 ± 0.40	0	0.57 ± 0.22
High ΔM	3	3.93 ± 0.16	-	-	-	-	0	0.58 ± 0.16
Combined	20	29.2 ± 1.8	16	15.2 ± 1.5	6	13.3 ± 1.4	15	16.2 ± 1.5
Very low ΔM	18	19.0 ± 1.7	13	10.8 ± 1.3	5	6.64 ± 0.99	15	13.3 ± 1.4
Low ΔM	0	3.09 ± 0.56	4	3.38 ± 0.68	5	5.69 ± 0.88	1	1.88 ± 0.50
Medium ΔM	3	3.06 ± 0.39	0	0.255 ± 0.056	0	1.25 ± 0.37	0	0.36 ± 0.16
High ΔM	4	4.67 ± 0.23	-	-	-	-	0	0.503 ± 0.084
Combined	25	29.4 ± 1.8	17	14.1 ± 1.4	9	12.7 ± 1.3	16	15.8 ± 1.5
Very low ΔM	8	8.55 ± 0.75	8	4.88 ± 0.57	0	3.00 ± 0.45	7	5.99 ± 0.63
Low ΔM	0	1.35 ± 0.25	0	1.54 ± 0.31	1	2.48 ± 0.40	0	0.85 ± 0.22
Medium ΔM	0	1.40 ± 0.18	0	0.148 ± 0.027	2	0.58 ± 0.17	0	0.24 ± 0.07
High ΔM	2	2.27 ± 0.11	-	-	-	-	0	0.25 ± 0.04
Combined	10	13.39 ± 0.82	8	6.42 ± 0.64	2	5.70 ± 0.60	7	7.16 ± 0.67
Very low ΔM	46	53.6 ± 4.7	38	30.6 ± 3.6	15	18.8 ± 2.8	41	37.6 ± 4.0
Low ΔM	1	8.8 ± 1.7	8	10.4 ± 2.0	10	16.4 ± 2.5	1	5.4 ± 1.4
Medium ΔM	7	8.8 ± 1.1	0	1.15 ± 0.23	2	3.7 ± 1.0	0	1.32 ± 0.54
High ΔM	12	12.10 ± 0.31	-	-	-	-	0	1.46 ± 0.18
Combined	66	82.1 ± 5.1	46	41.0 ± 4.0	25	36.3 ± 3.8	42	44.8 ± 4.2

Table 3: Number of observed events, N_{D}, and SM background expectations, N_{SM}, for the stop and sbottom selections. The contribution of two-fermion ($\mathrm{q\bar{q}}$, $\tau^+\tau^-$), four-fermion ($\mathrm{W^+W^-}$, $\mathrm{W^\pm e^\mp}\nu$, ZZ, $\mathrm{Ze^+e^-}$) and two-photon ($\mathrm{e^+e^-q\bar{q}}$, $\mathrm{e^+e^-}\tau^+\tau^-$) processes are given separately. The quoted errors are due to MC statistics only.

Channel	N_{D}	$N_{\mathrm{two-fermion}}$	$N_{\mathrm{four-fermion}}$	$N_{\mathrm{two-photon}}$	N_{SM}
$\tilde{\mathrm{t}}_1 \to \mathrm{c}\tilde{\chi}^0_1$	66	0.44 ± 0.22	20.87 ± 0.37	61.0 ± 5.1	82.1 ± 5.1
$\tilde{\mathrm{t}}_1 \to \mathrm{b}\ell\tilde{\nu}$	46	0.94 ± 0.35	1.71 ± 0.10	38.5 ± 4.0	41.0 ± 4.0
$\tilde{\mathrm{t}}_1 \to \mathrm{b}\tau\tilde{\nu}$	25	0.56 ± 0.27	1.92 ± 0.11	34.0 ± 3.8	36.3 ± 3.8
$\tilde{\mathrm{b}}_1 \to \mathrm{b}\tilde{\chi}^0_1$	42	0.37 ± 0.22	2.77 ± 0.13	41.8 ± 4.2	44.8 ± 4.2
Total	129	1.41 ± 0.42	23.06 ± 0.39	112.5 ± 6.9	136.7 ± 6.9

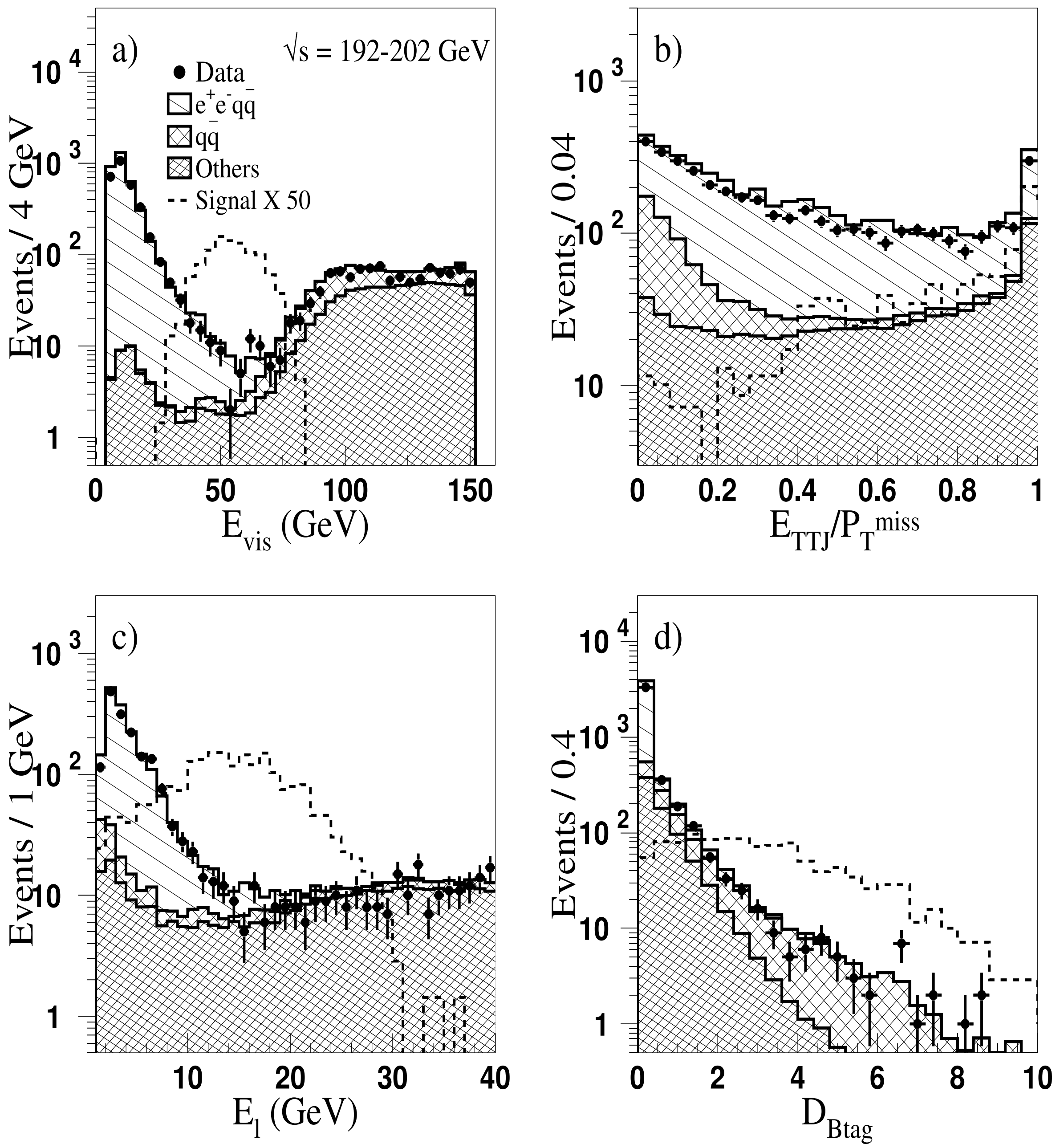

Figure 1: Distributions of a) E_{vis}, b) $E_{\mathrm{TTJ}}/P_{\mathrm{T}}^{\mathrm{miss}}$ (see text), c) the most energetic lepton energy E_{ℓ}, and d) b-tagging event discriminant D_{Btag} for data and MC events after preselection. Contributions from $\mathrm{e^+e^-q\bar{q}}$, $\mathrm{q\bar{q}}$ and other backgrounds, dominated by $\mathrm{W^+W^-}$ production, are given separately. The distributions for expected signal events of $\tilde{\mathrm{t}}_{\mathrm{L}} \to \mathrm{c}\tilde{\chi}_1^0$ (a,b), $\tilde{\mathrm{t}}_{\mathrm{L}} \to \mathrm{b}\ell\tilde{\nu}$ (c) and $\tilde{\mathrm{b}}_{\mathrm{L}} \to \mathrm{b}\tilde{\chi}_1^0$ (d) with $M_{\tilde{\mathrm{q}}}$=90 GeV, $M_{\tilde{\chi}_1^0}$=60 GeV are also shown.

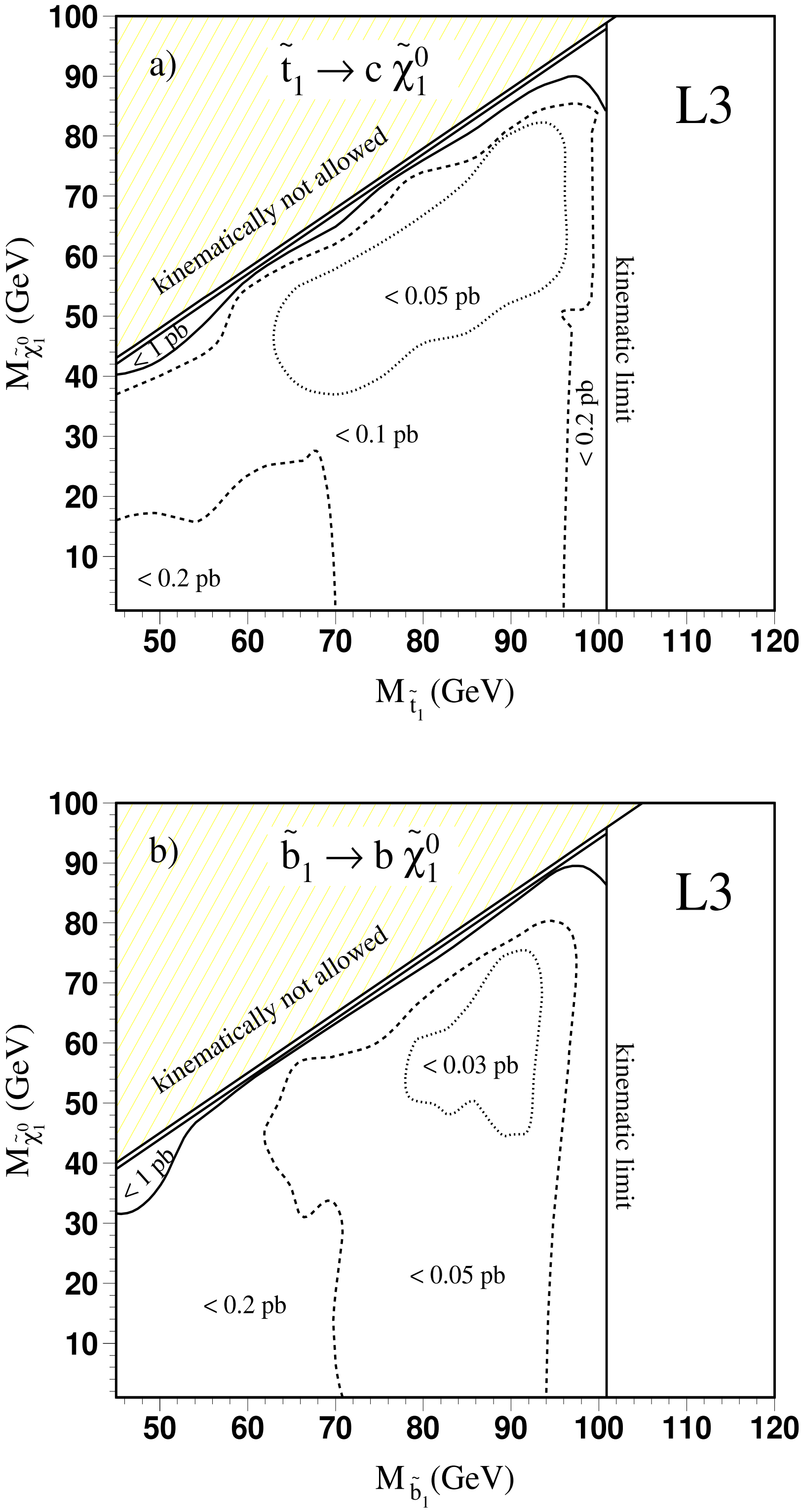

Figure 2: Upper limits on a) $e^+e^- \to \tilde{t}_1\bar{\tilde{t}}_1 \to c\tilde{\chi}^0_1\bar{c}\tilde{\chi}^0_1$ and b) $e^+e^- \to \tilde{b}_1\bar{\tilde{b}}_1 \to b\tilde{\chi}^0_1\bar{b}\tilde{\chi}^0_1$ production cross section times branching ratio. Limits are obtained by combining the results at centre of mass energies of $\sqrt{s}$=161–172 GeV, 183 GeV, 189 GeV and 192–202 GeV.

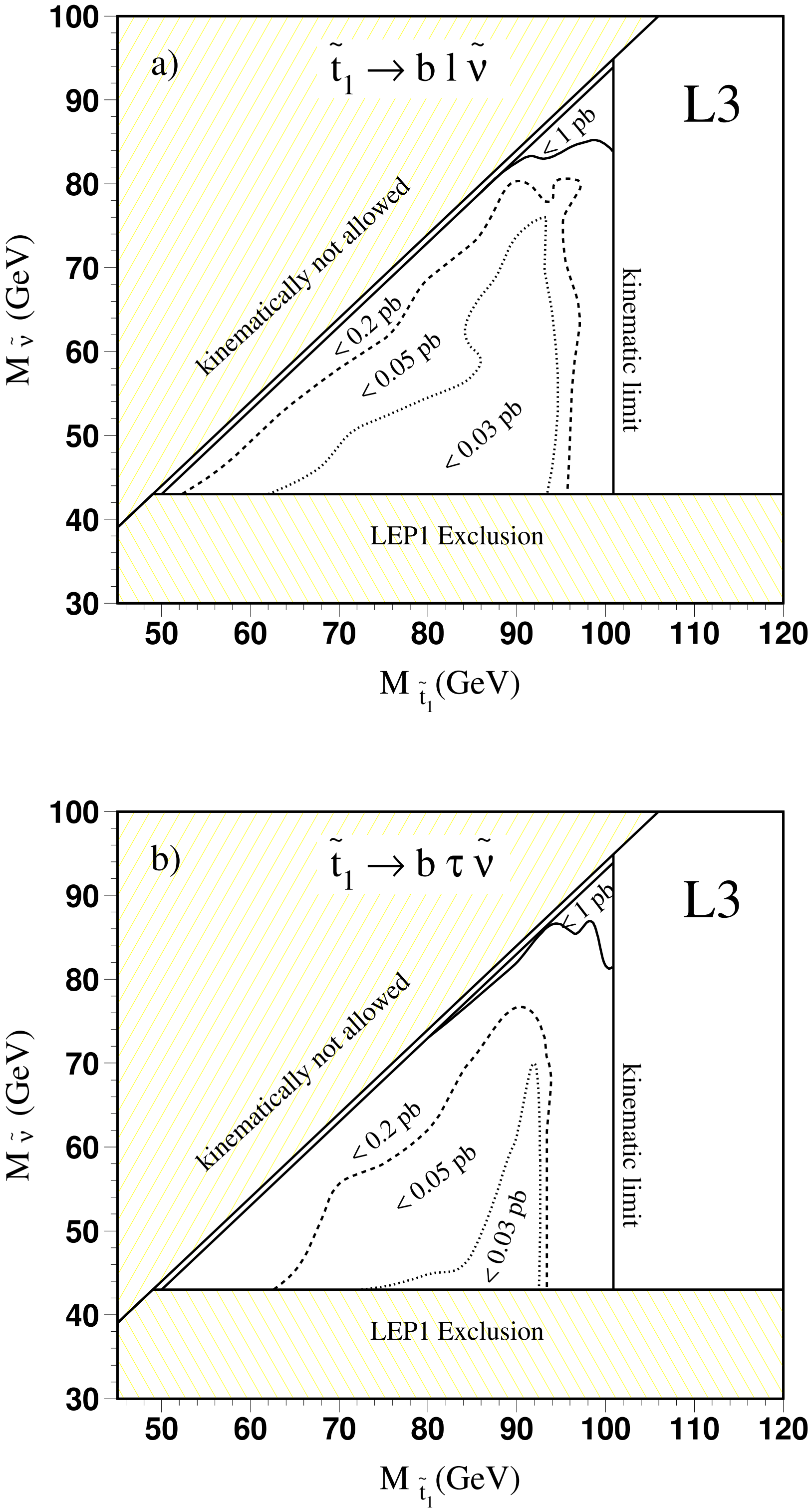

Figure 3: Upper limits on a) $e^+e^- \rightarrow \tilde{t}_1\bar{\tilde{t}}_1 \rightarrow b\ell^+\tilde{\nu}\bar{b}\ell^-\tilde{\nu}$, $\ell = e, \mu, \tau$ assuming lepton universality and b) $e^+e^- \rightarrow \tilde{t}_1\bar{\tilde{t}}_1 \rightarrow b\tau^+\tilde{\nu}\bar{b}\tau^-\tilde{\nu}$ production cross section times branching ratio. Limits are obtained by combining the results at centre of mass energies of $\sqrt{s}$=161–172 GeV, 183 GeV, 189 GeV and 192–202 GeV.

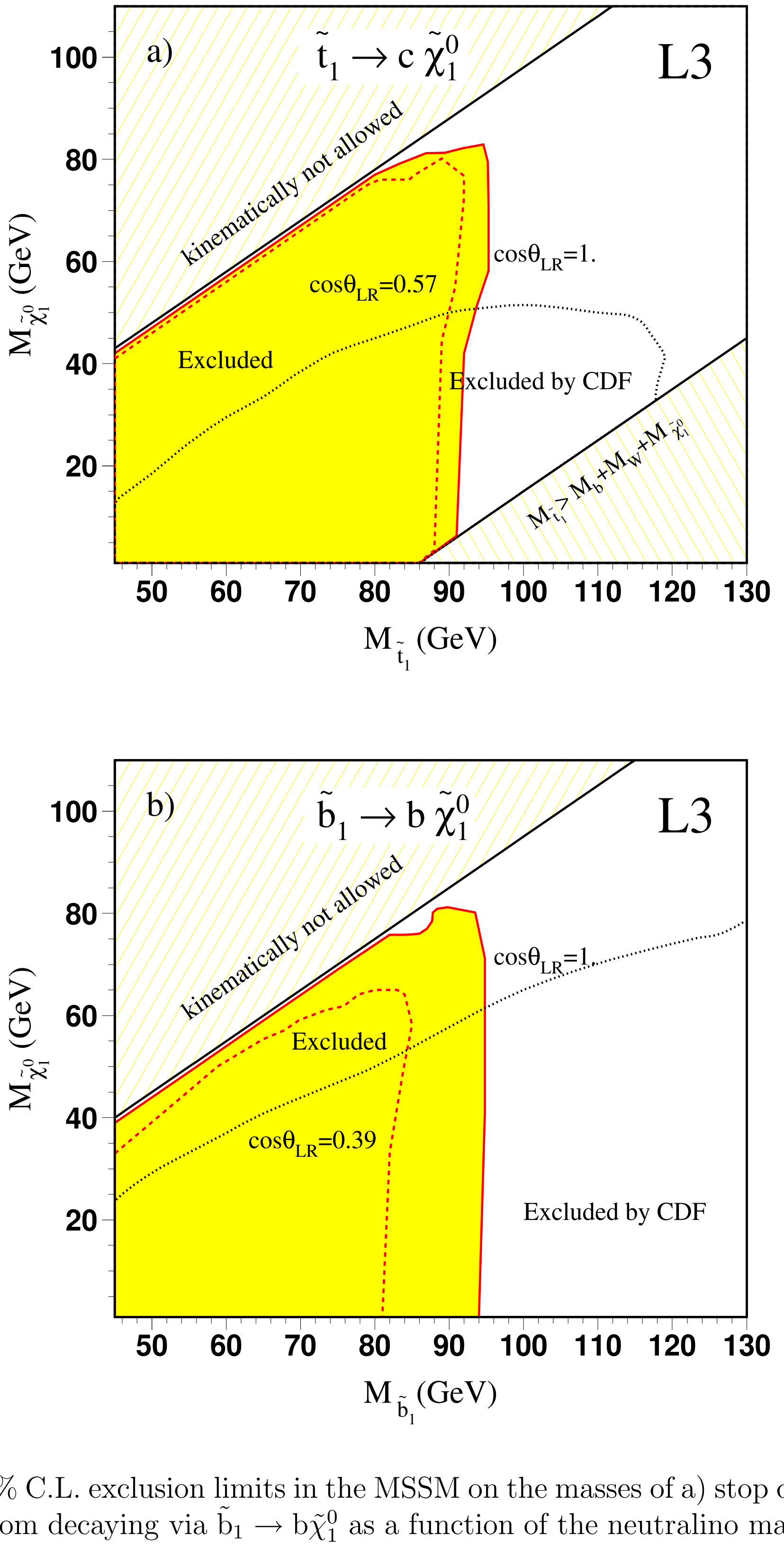

Figure 4: 95% C.L. exclusion limits in the MSSM on the masses of a) stop decaying via $\tilde{t}_1 \rightarrow c\tilde{\chi}^0_1$ and b) sbottom decaying via $\tilde{b}_1 \rightarrow b\tilde{\chi}^0_1$ as a function of the neutralino mass with maximal and minimal cross section assumptions. For comparison results obtained by CDF [6] experiment are also shown.

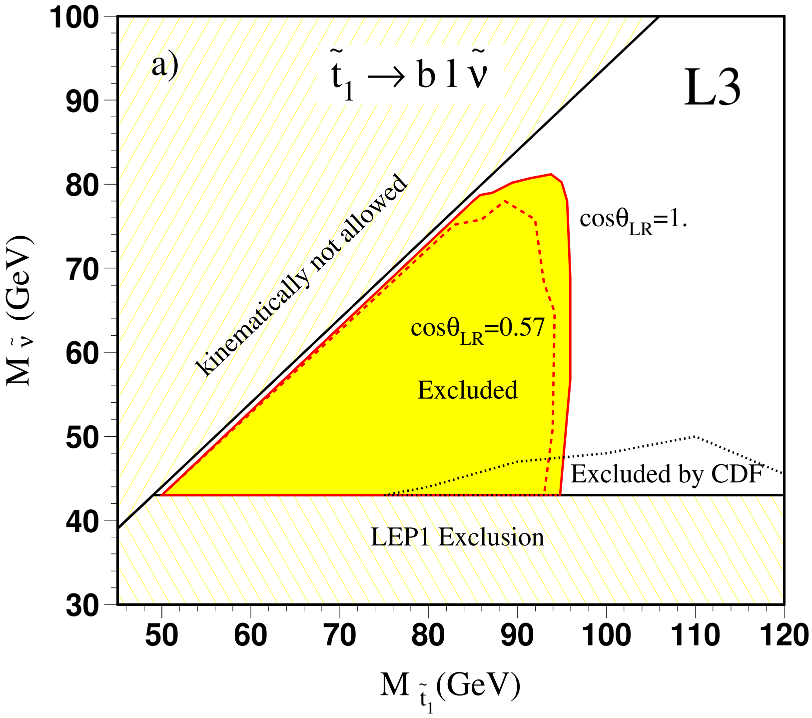

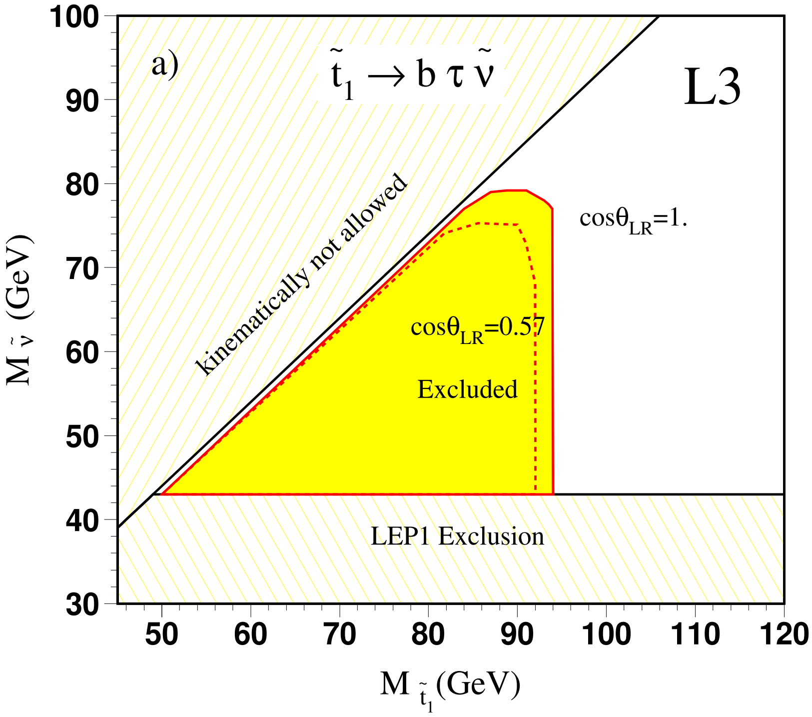

Figure 5: 95% C.L. exclusion limits in the MSSM on the mass of stop decaying via a) $\tilde{t}_1 \to b\ell\tilde{\nu}$, $\ell = e, \mu, \tau$ with equal probability and b) $\tilde{t}_1 \to b\tau\tilde{\nu}$, as a function of the sneutrino mass with maximal and minimal cross section assumptions. The sneutrino mass limit obtained at LEP1 is also shown. For comparison exclusion obtained by CDF experiment in $\tilde{t}_1 \to b\ell\tilde{\nu}$, $\ell = e, \mu, \tau$ searches is presented [26].

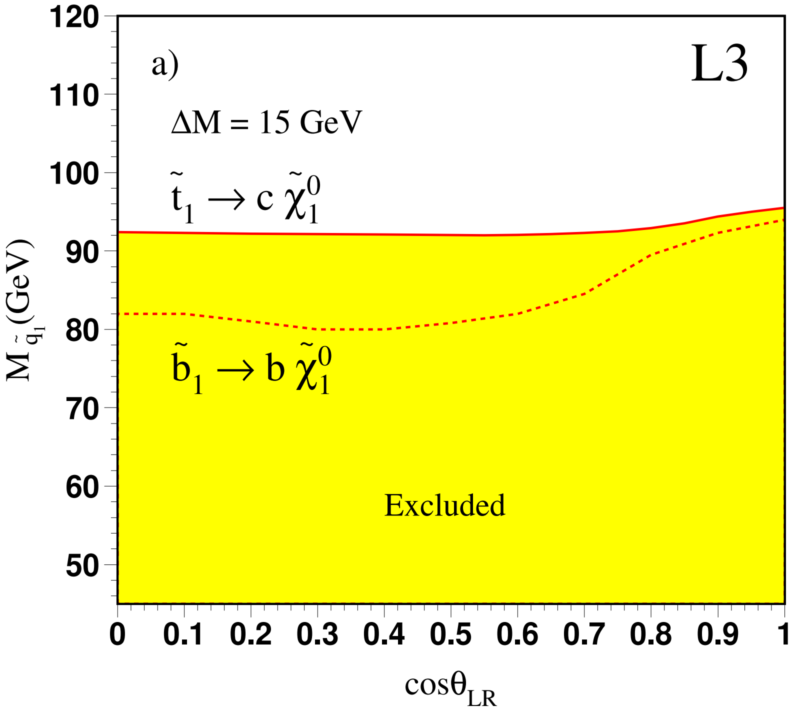

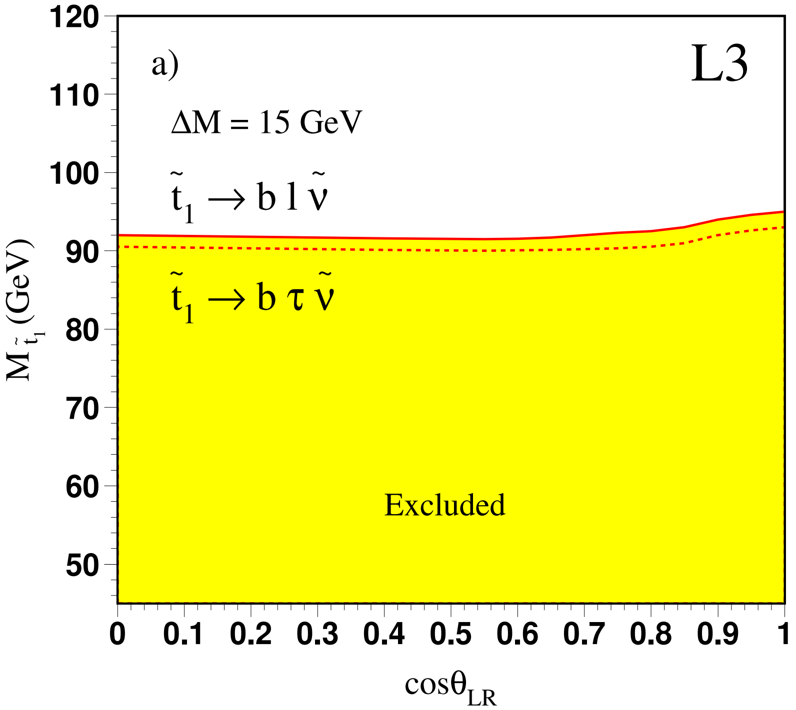

Figure 6: 95% C.L. exclusion limits in the MSSM as a function of the mixing angle $\cos\theta_{\rm LR}$ for the a) stop decaying via $\tilde{\rm t}_1 \to {\rm c}\tilde{\chi}^0_1$ (solid line) and sbottom decaying via $\tilde{\rm b}_1 \to {\rm b}\tilde{\chi}^0_1$ (dashed line), b) stop decaying via $\tilde{\rm t}_1 \to {\rm b}\ell\tilde{\nu}$, $\ell = e, \mu, \tau$ with equal probability (solid line) and $\tilde{\rm t}_1 \to {\rm b}\tau\tilde{\nu}$ (dashed line).

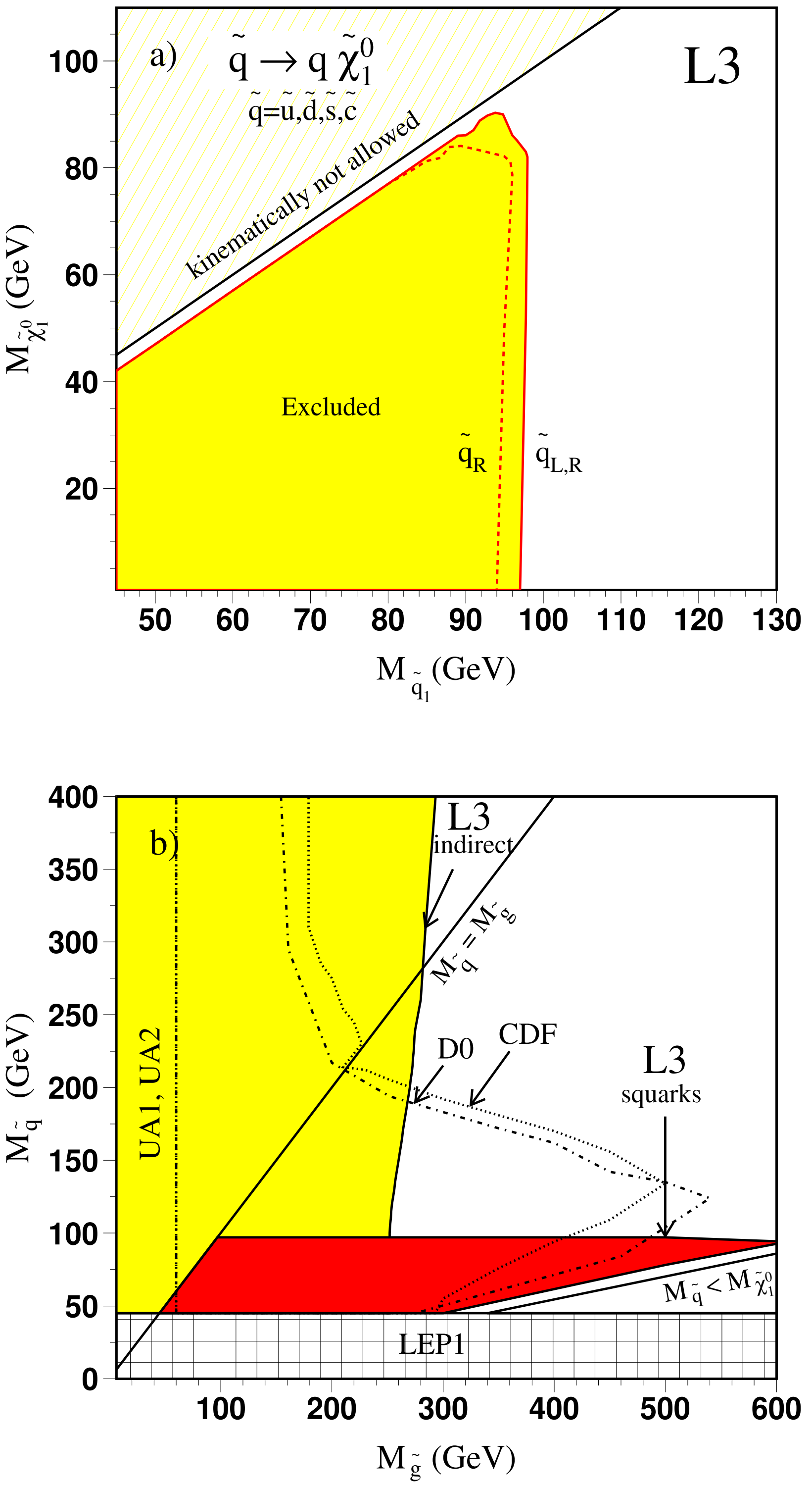

Figure 7: a) 95% C.L. exclusion limits in the MSSM on the masses of the degenerate squarks decaying via $\tilde{q} \rightarrow q\tilde{\chi}^0_1$. b) Excluded regions in the ($M_{\tilde{g}}$, $M_{\tilde{q}}$) plane. The dark shaded area is excluded from the search of squarks of the first two families, assuming the mass degeneracy among different flavours and between "left" - "right" squarks. The light shaded area illustrates indirect limits on the gluino mass, derived from the chargino, neutralino and scalar lepton searches. The regions excluded by the CDF and D0 collaborations [27] are valid for $\tan\beta = 4$ and $\mu = -400$ GeV. The exclusions obtained by the UA1 and UA2 [28] collaborations are also shown.